Novel Approach To Predicting P450-Mediated Drug Metabolism: Development of a Combined Protein and Pharmacophore Model for CYP2D6

Marcel J. de Groot,*,‡ Mark J. Ackland,† Valerie A. Horne,‡ Alexander A. Alex,‡ and Barry C. Jones†

Departments of Computational Chemistry and Drug Metabolism, Pfizer Central Research, Sandwich, Kent CT13 9NJ, United Kingdom

Received December 4, 1998

A combined protein and pharmacophore model for cytochrome P450 2D6 (CYP2D6) has been derived using various computational chemistry techniques. A combination of pharmacophore modeling (using 40 substrates), protein modeling, and molecular orbital calculations was necessary to derive a model which incorporated steric, electronic, and chemical stability properties. The initial pharmacophore and protein models used to construct the combined model were derived independently and showed a high level of complementarity. The combined model is in agreement with experimental results concerning the substrates used to derive the model, with site-directed mutagenesis data available for the CYP2D6 protein, and takes into account the site-directed mutagenesis results for a variety of other 2-family P450s.

Introduction

Cytochromes P450 (P450s) constitute a large superfamily of heme-containing enzymes, capable of oxidizing and reducing a variety of substrates. Cytochrome P450 2D6 (CYP2D6)[1] is a polymorphic member of the P450 superfamily which is absent in 5−9% of the Caucasian population. Several inactivating alleles have been reported,[2] which result in a deficiency in drug oxidation known as the debrisoquine/sparteine polymorphism, affecting the metabolism of numerous drugs. The known substrates of CYP2D6 represent a variety of chemical structures, common characteristics being the presence of at least one basic nitrogen atom, a distance of 5 or 7 Å between the basic nitrogen atom and the site of oxidation, a flat hydrophobic area near the site of oxidation, and a negative molecular electrostatic potential (MEP) above the planar part of the molecule.[3−5] However, several substrates with a distance of approximately 10 Å between the basic nitrogen atom and the site of oxidation are known.

Theoretical models capable of predicting the possible involvement of CYP2D6 in the metabolism of drugs or drug candidates are important tools for use in drug discovery and drug development. Several pharmacophore models have been published based on the chemical structure of a variety of substrates[3,5−10] or reversible inhibitors of CYP2D6.[4]

Homology modeling has been used to develop structures of P450s for which sequence information is available, but X-ray structures are lacking. These models have to be verified by either crystallization or site-directed mutagenesis experiments.[11] As yet crystal structures have been resolved for only four bacterial, soluble P450s: CYP101 ($P450_{cam}$),[12,13] CYP102 ($P450_{BM3}$),[14,15] CYP107A ($P450_{eryF}$),[16,17] and CYP108 ($P450_{terp}$),[18] and a fungal P450 (CYP55, $P450_{nor}$) from *Fusarium oxysporum*.[19,20] The crystal structure of CYP107A[17] shows some significant differences compared to the crystal structures of CYP101, CYP102, and CYP108, especially in the regions of the A-, B′-, F-, and G-helices.[17] The crystal structure of CYP55 is different from the structures of the bacterial P450s as the active site region is wide open, reflecting the difference in activity (reduction of nitric oxide instead of monooxygenation activity).[20,21]

In the literature, several homology models have been reported of eukaryotic P450s based on the crystal structure of either CYP101 or CYP102 or a combination of CYP101, CYP102, and CYP108. For a recent review of these models, see de Groot and Vermeulen.[22] CYP102 is considered to provide the most useful structural information for homology studies on eukaryotic P450s, since this well-characterized and crystallized bacterial enzyme belongs to the class II P450s[14] to which many eukaryotic P450s belong.

A variety of three-dimensional representations of the active site of CYP2D6 have been constructed using homology modeling techniques.[23−28] One specific amino acid, Asp301, was proposed to be a crucial amino acid in the active site of CYP2D6, probably by forming an ionic hydrogen bond with basic nitrogen atoms of substrates (or inhibitors),[8,23,25,26,28] a proposal which has been supported by recent site-directed mutagenesis experiments.[29]

The aim of the present study is to derive a three-dimensional model for CYP2D6 and its substrates, based on the combination of (a) a homology model constructed using the crystal structures of CYP101, CYP102, and CYP108, (b) a pharmacophore model, and (c) molecular orbital (MO) calculations on the substrates, metabolic intermediates, and products, which will enable us to rationalize and more specifically to predict CYP2D6-mediated metabolism.

This methodology offers a more complete understanding of the CYP2D6 active site and its interactions with substrates than each of these approaches alone, since it takes into account the most reactive sites in the substrate as well as the conformational and stereochemical constraints imposed by the protein active site.

* Corresponding author.
‡ Department of Computational Chemistry.
† Department of Drug Metabolism.

10.1021/jm981118h CCC: $18.00
Published on Web 04/17/1999

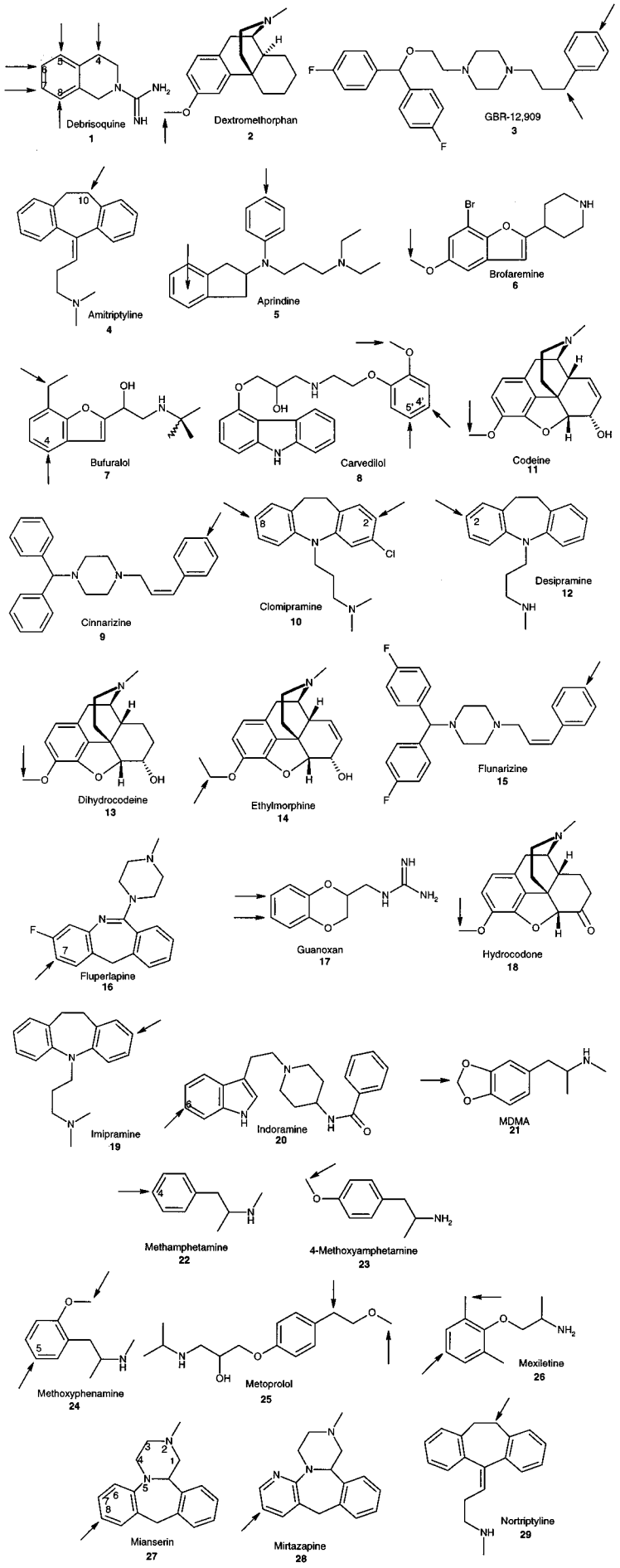
Debrisoquine
1
Dextromethorphan
2
GBR-12,909
3
Amitriptyline
4
Aprindine
5
Brofaremine
6
Bufuralol
7
Carvedilol
8
Codeine
11
Cinnarizine
9
Clomipramine
10
Desipramine
12
Dihydrocodeine
13
Ethylmorphine
14
Flunarizine
15
Fluperlapine
16
Guanoxan
17
Hydrocodone
18
Imipramine
19
Indoramine
20
MDMA
21
Methamphetamine
22
4-Methoxyamphetamine
23
Methoxyphenamine
24
Metoprolol
25
Mexiletine
26
Mianserin
27
Mirtazapine
28
Nortriptyline
29

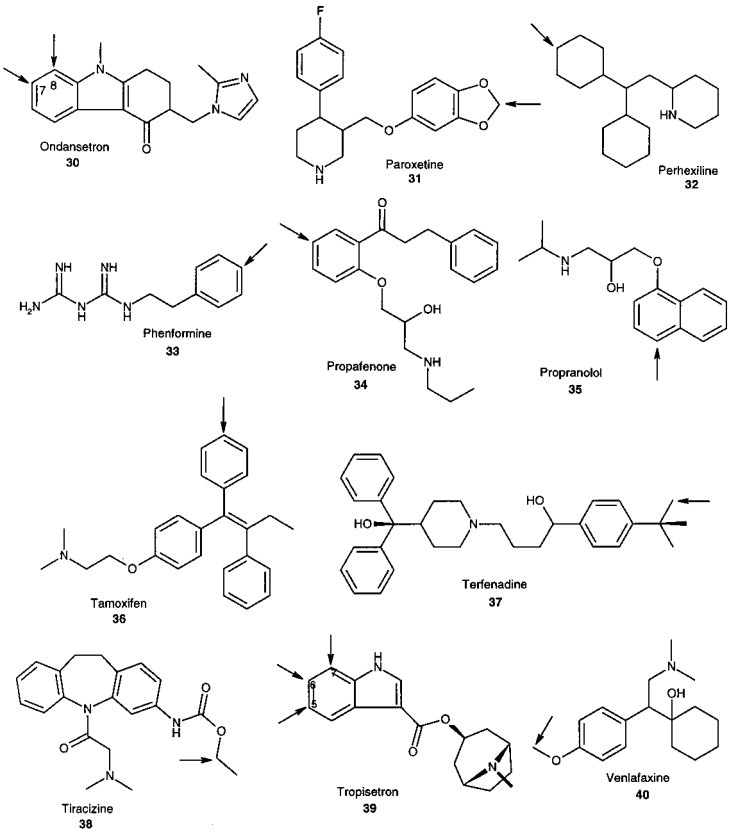

Figure 1. Substrates of CYP2D6 used to construct the combined model. Sites of metabolism under investigation are marked with an arrow.

The independent generation of the pharmacophore and protein models offers the opportunity to compare and contrast as well as "cross-validate" the approaches. Furthermore, when using the model for predictions concerning metabolism catalyzed by CYP2D6 of new compounds, for which no information is available in relation to the actual site of oxidation, the MO calculations will indicate the electronically most likely sites of oxidation which can be used to guide the modeling efforts.

Computational Methods

Construction of a Pharmacophore Model for Substrates of CYP2D6. A series of 57 metabolic pathways of 40 substrates known to be metabolized by human CYP2D6 were obtained, together with information concerning their sites of oxidation (see Figure 1 and Table 1). Where possible structures for modeling were obtained from the Cambridge Structural Database (CSD),[30] but otherwise the structures were built using SPARTAN.[31] For each of the substrates a conformational search followed by an energy minimization was performed[32] using the AM1 method[33] in SPARTAN.[31] To construct the template, debrisoquine (**1**) and dextromethorphan (**2**) were selected in which the distance between the site of oxidation and the basic nitrogen atom was fixed at approximately 5 and 7 Å, respectively.[34] GBR-12,909 (**3**) was added to this set of template molecules because of the size of this compound. The oxidation site of debrisoquine was then fitted onto the oxidation site of dextromethorphan while keeping the conformation near the oxidation site coplanar. Each substrate was then overlaid using the aforementioned criteria onto either debrisoquine or dextromethorphan depending on whether it was a 5 or 7 Å substrate using the "MULTIFIT" method in SYBYL.[35] Where possible structures containing bulky groups attached to the basic nitrogen (e.g., compound **35**) were oriented vertically away from the template on the basis of a possible lipophilic pocket in this region of space within the active site. All substrates had a final fit that was within 10 kcal/mol of their respective global minimum energies according to the SYBYL force field.[35] Only three compounds (compounds **1**, **24**, and **26**) have a distance around 5 Å (4.5−5.5 Å) between the site of oxidation and the basic nitrogen atom. Not all substrates modeled were able to conform to the 5 or 7 Å model. Compounds **6**, **25**, and **36**−**39** display a distance of approximately 10 Å (9.4−10.7 Å) between the basic nitrogen atom and the site of oxidation. This group of substrates was added to the pharmacophore after combination of the pharmacophore and protein models, as these substrates could not interact with Asp301 as the 5 and 7 Å substrates could. All other compounds are classified as '7 Å substrates' (6.4−8.8 Å).

Construction of a Homology Model for CYP2D6. CYP101, CYP102, and CYP108 were used as templates for the CYP2D6 protein model.[36] CYP107 was not included after inspection of the coordinates indicated that it has a very similar structure to CYP101 in all but two surface loops and the B′ region,[16] where the differences would not have led to an enhancement of the model. The consensus homology modeling program Modeler (as implemented in Quanta97),[37] has been applied to an alignment similar to that of de Groot et al.[26,38] (Figure 2), which is continuous and includes the A-, D-, E-, H-, and K′-helices that were not present in the previous model.[26] The alignment in the β-sheet region at the C-terminus of the protein was adjusted from that of de Groot et al.[26] to significantly improve the model by restoring the β-sheet structure of this region. This resulted in Phe481 rather than Phe483 being oriented toward the active site. Site-directed mutagenesis work[39] corroborates Phe481 and not Phe483 as being involved in interactions in the active site of CYP2D6, although recently Phe483 was indicated to be important in acquiring the ability to metabolize testosterone.[40]

Our initial models were constructed using the complete structures of CYP101, CYP102, and CYP108 as templates (consensus models). These models most closely follow CYP102 in the B′-region resulting in Phe120 of CYP2D6 being placed over Phe87 of CYP102. However, Phe120 in this orientation partially occludes Asp301 with which most CYP2D6 substrates

Table 1. CYP2D6 Substrates Used in the Model, Their Metabolic Pathways, and Their (Fitted) Distances between Site(s) of Oxidation and Basic Nitrogen Atom

name	pathway	distance (Å)	ref
1, debrisoquine	4-hydroxylation	4.76[a]	52, 53
	5-hydroxylation	6.42	53
	6-hydroxylation	6.94	53
	7-hydroxylation	6.36	53
	8-hydroxylation	5.36[a]	53
2, dextromethorphan	O-demethylation	8.06	54
3, GBR-12,909	benzylic hydroxylation	6.75	9
	aromatic hydroxylation[43]	7.61	9
4, amitriptyline	10-hydroxylation	7.16	55
5, aprindine	aromatic hydroxylation	7.46	56
	fused ring hydroxylation	8.69	56
6, brofaremide	O-demethylation	9.34	57
7, bufuralol	1′-hydroxylation	7.07	7, 58
	4-hydroxylation	7.68	7, 58
8, carvedilol	4′-hydroxylation	7.06	59
	5′-hydroxylation	6.74	59
	O-demethylation	7.34	59
9, cinnarizine	aromatic hydroxylation	7.63	60
10, clomipramine	2-hydroxylation	8.63	61
	8-hydroxylation	8.57	61
11, codeine	O-demethylation	8.15	62
12, desipramine	2-hydroxylation	7.86	63
13, dihydrocodeine	O-demethylation	8.17	64
14, ethylmorphine	O-demethylation	8.05	65
15, flunarizine	aromatic hydroxylation	7.67	60
16, fluperlapine	7-hydroxylation	8.79	66
17, guanoxan	7-hydroxylation	8.34	67
	8-hydroxylation	7.83	67
18, hydrocodone	O-demethylation	8.09	68
19, imipramine	aromatic hydroxylation	8.46	63
20, indoramine	6-hydroxylation	7.78	69
21*R*, MDMA	O-demethylation	7.09	70
21*S*, MDMA	O-demethylation	6.76	70
22, methamphetamine	4-hydroxylation	7.02	71
23, 4-methoxy-amphetamine	O-demethylation	6.66	72
24, methoxyphenamine	5-hydroxylation	4.60[a]	73
	O-demethylation	4.73[a]	73
25, metoprolol	benzylic hydroxylation	9.79[b]	58
	O-demethylation	10.65[b]	58
26*R*, mexiletine	aromatic hydroxylation	7.47	74
	benzylic hydroxylation	4.58[a]	74
26*S*, mexiletine	aromatic hydroxylation	7.49	74
	benzylic hydroxylation	5.05[a]	74
27, mianserine	5-hydroxylation	7.16	75
28, mirtazapine	aromatic hydroxylation	7.15	76
29, nortriptyline	benzylic hydroxylation	6.87	55, 77
30, ondansetron	7-hydroxylation	8.38	78
	8-hydroxylation	7.98	78
31, paroxetine	O-demethylation	8.08	79
32, perhexiline	ring hydroxylation	7.00	80, 81
33, phenformine	aromatic hydroxylation	7.45	82
34, propafenone	aromatic hydroxylation	8.49	83, 84
35, propranolol	aromatic hydroxylation	7.98	85, 86
36, tamoxifen	4-hydroxylation	10.02[b]	87, 88
37, terfenadine	*tert*-butyl hydroxylation	9.80[b]	89
38, tiracizine	O-demethylation	9.71[b]	90
39, tropisetron	5-hydroxylation	9.81[b]	78
	6-hydroxylation	9.93[b]	78
	7-hydroxylation	10.07[b]	78
40, venlafaxine	O-demethylation	7.64	91

[a] 5 Å substrate (interacting with Asp301). [b] 10 Å substrate (interacting with Glu216 instead of Asp301). All other compounds are 7 Å substrates (interacting with Asp301).

are thought to interact.[23−29] The model of de Groot et al.[26] has the B′-to-C-helix region based only on CYP108, resulting in Phe120 being placed in an adjacent hydrophobic pocket lined by Phe275, Phe290, Ile297, and Val298. This leaves the active site above heme pyrrole rings A and D[41] more open to accommodate the CYP2D6 substrates, some of which are bulkier than the fatty acids metabolized by CYP102.

As described by de Groot et al.,[26] a template was selected for each structural element from either CYP101, CYP102, or CYP108 (see Table 2) for further homology modeling of CYP2D6. For the regions not present in the model of de Groot et al.,[26] a consensus of the three cytochrome crystal structures was used. The heme moiety of CYP108 was used, with the two propionyl groups oriented to the proximal side of the heme, interacting with Arg132, His376, Ser413, and Arg441. The structures of CYP101 and CYP102 have the heme pyrrole ring A propionate as in CYP108 but the heme pyrrole ring D propionate orientated on the distal side of the heme. The propionate carboxylate moieties can make the same interactions in either case, with water molecules necessary for a good hydrogen bond interaction between the heme pyrrole ring D propionate and His376.

A set of 20 Modeler models was produced using a template from either CYP101, CYP102, or CYP108 or a consensus for each structural region (see Table 2), applying the alignment shown in Figure 2. The best of these CYP2D6 protein models was selected for combination with the simultaneously developed pharmacophore model. Selection was based on a Procheck[42] analysis of stereochemical quality, and a visual inspection in Quanta97[37] to assess the orientation of Phe120 and Phe481 and the orientation of the amino acids involved in hydrogen bonds with the heme propionate moieties.

Lewis et al.[28] recently suggested the involvement of Glu216 in binding and orienting large substrates in the CYP2D6 active site. For the set of substrates used for our model, this amino acid might be involved in binding compounds **3**,[43] **6**, **25**, and **36**−**39** in the active site of our model, forming an additional hydrogen bond. Some of these substrates are unable to interact with Asp301 and could only be docked into the protein using Glu216 as an alternative interaction site for the basic nitrogen atoms in these compounds.

Molecular Orbital (MO) Calculations on CYP2D6 Substrates. As indicated above, for each of the substrates (Figure 1) a conformational search followed by an energy minimization was performed[32] using the AM1 method[33] in SPARTAN.[31] Starting from the lowest energy-minimized conformation of the molecule, all likely radicals and hydroxylated products and the radical cation were generated and geometry-optimized.[32] For each substrate the chemically and kinetically most likely products were compared with the experimentally observed metabolic products. Figure 3 shows a representative example of the relative stabilities of the possible hydroxylated products of compound **2** (dextromethorphan).

The MO calculations will become more important when predictions based on the model are made. In this case no experimental information is available for the compound under investigation, and the MO results for the various possible products will be used to guide the modeling.

After combination of the pharmacophore and homology model and minimization of the substrates in the presence of the protein, a similar AM1 geometry optimization was performed on the geometry of the substrate resulting from this minimization in the protein.

Combination of the Pharmacophore and Homology Models for CYP2D6 with the MO Calculations. The MO results were used to check the energies of the known hydroxylated products relative to the most stable hydroxylated products. This process will become more important when predictions are made using this model.

The protein model for CYP2D6 was reoriented in space using Quanta97.[37] The plane of the heme was defined in the *XY*-plane with the center of the heme at the origin, the proximal side of the heme in the $+Z$-direction, and the propionate side chains of the heme in the $+X$-direction. Then the derived CYP2D6 pharmacophore model was oriented into the active site of the CYP2D6 protein model using SYBYL.[35]

Initially the complete set of 5 and 7 Å substrates was oriented within the CYP2D6 protein model without changing the orientations of the substrates relative to each other. The set of 5 and 7 Å substrates was oriented with the site of oxidation at approximately 3−3.5 Å above the iron atom of the heme and the basic nitrogen atom oriented toward the side chain of Asp301, while avoiding steric clashes with the other amino acids lining the interior of the active site. The phar-

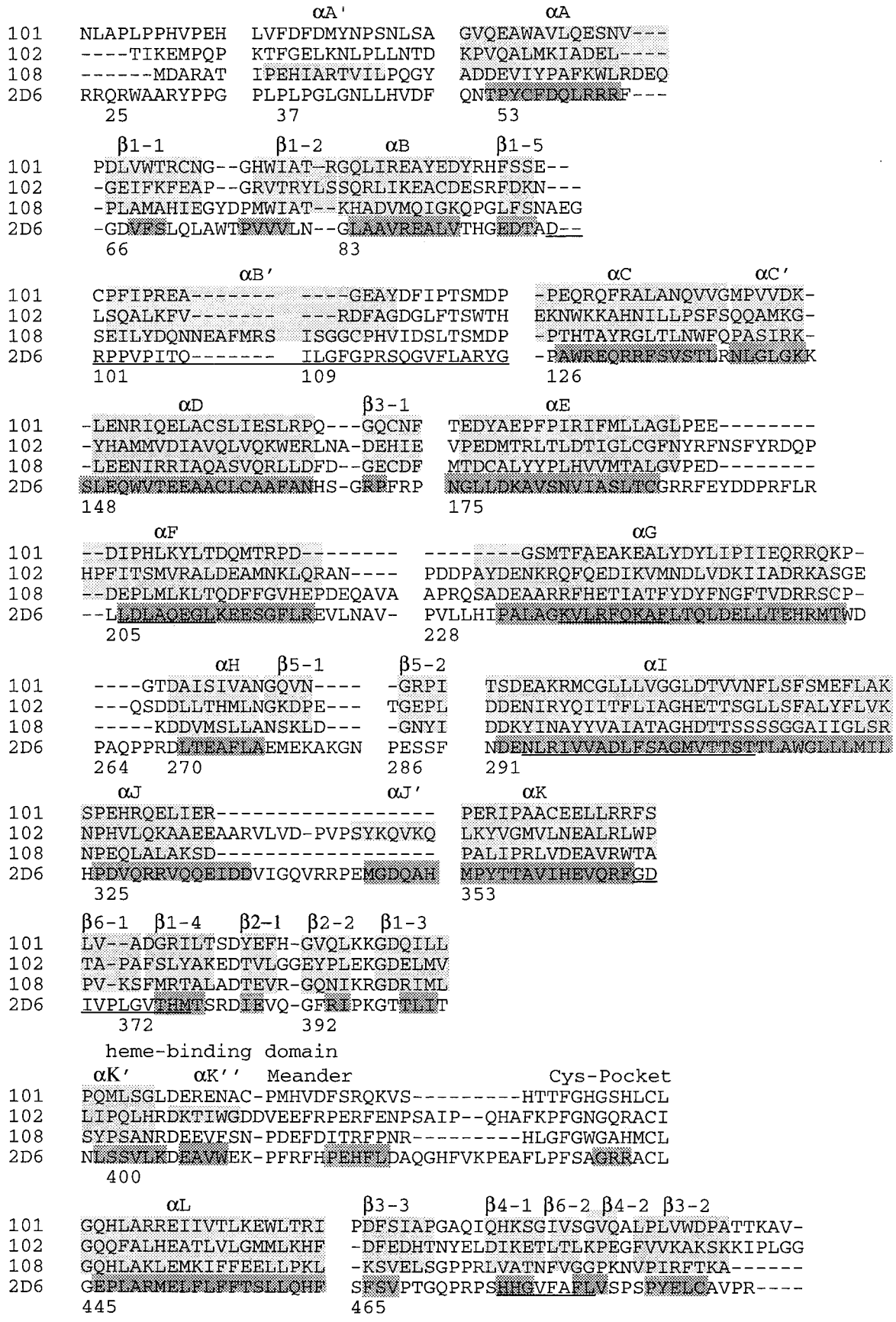

Figure 2. Alignment of CYP2D6 with CYP101, CYP102, and CYP108, based for a large part on a previous multialignment of 66 CYP2-family P450s with the bacterial P450s.[26,38] Secondary structure elements present in the X-ray structures are indicated in light gray and are named according to the naming scheme used by Hasemann et al.[51] Secondary structure elements present in the CYP2D6 model are depicted in dark gray. Substrate recognition site regions (SRS) as derived by Gotoh[48] are underlined.

Table 2. Template Choice for the Various Regions of the CYP2D6 Protein Model

main structural region	start	end	CYP template(s)
A-helix	Arg25	Phe65	consensus
β-sheet	Gly66	Asn82	108
B-helix	Gly83	Asp100	101
B′-helix N-terminal part	Arg101	Gln108	101
B′-helix C-terminal part	Ile109	Gly125	108
C- and C′-helices	Pro126	Lys147	108
D-helix	Ser148	Arg173	consensus
E-helix	Pro174	Arg204	consensus
F-helix	Leu205	Val227	102
G-helix	Pro228	Asp263	102
H-helix	Pro264	Asn285	consensus
β-sheet	Pro286	Asn291	102
I-helix	Asp292	His324	102
J-helix	Pro325	Asn341	102
J′-helix	Val342	Met353	102
K-helix	Pro354	Pro371	102
β-sheet region	Leu372	Leu399	102
heme-binding domain	Ser400	Leu444	102
L-helix	Gly445	Phe464	102
β-sheet region	Ser465	Arg497	102
heme moiety			108

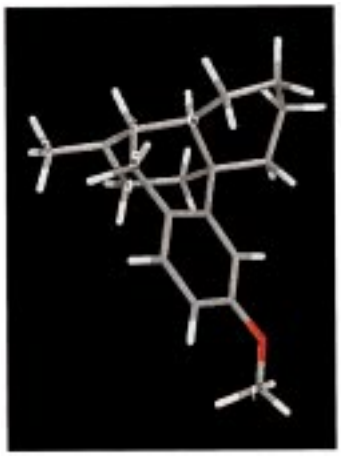

Site	ΔE (kcal/mol)	distance (Å)
1	0.0	7.8
2	8.6	1.4
3	16.6	1.5
4	10.2	1.5
5	12.4	2.6
6	17.4	2.5

Figure 3. Relative stabilities of the possible hydroxylated products of compound **2** (dextromethorphan). The energies are relative to the energy of the most stable hydroxylated product (in this instance site 1, resulting in O-demethylation, the observed metabolic product for this substrate). The distances between the basic nitrogen atom and the site of oxidation are also shown.

macophore model fitted (almost) perfectly in the protein model although the two models were derived independently, thereby validating each other. The orientation of compound **2** in the active site of the protein model for CYP2D6 is shown in Figure 4, left. The 10 Å substrates **6**, **25**, and **36**−**39** were then added, guided by the extending 7 Å substrate **3**.[43]

In the next step each individual substrate was energy-minimized within the active site using SYBYL.[35] In this minimization only amino acids Glu216, Asp301, and Phe481 (experimentally identified as amino acids responsible for interactions with substrates) and the substrate were free to minimize, with two distance constraints[44] to ensure known interactions are preserved. The orientation of compound **2** in the active site of the protein model for CYP2D6 after this protein minimization step is shown in Figure 4, right.

Results and Discussion

The set of 40 compounds (Figure 1) could be accommodated in a pharmacophore model using one site of oxidation and three different positions for the basic nitrogen atoms: one at 5 Å (4.5−5.5 Å), a second at 7 Å (6.4−8.8 Å), and a third at 10 Å (9.4−10.7 Å) from the site of oxidation. The basic nitrogen atoms of the 5 and 7 Å substrates can interact with Asp301, while the basic nitrogen atoms of the 10 Å substrates can interact with Glu216. Only three compounds are classified as 5 Å substrates (compounds **1** (4- and 8-hydroxylation), **24**, and **26** (benzylic hydroxylation)), while six compounds were classified as 10 Å substrates (**6**, **25**, and **36**−**39**). All other compounds are 7 Å compounds. Taking into account that most CYP2D6 substrates are 7 Å compounds, this might suggest that 5 Å compounds bind in a similar manner as the 7 Å substrates with a water molecule spanning the distance between the basic nitrogen atom and the carboxylic acid side chain of Asp301 instead of two different binding modes as used here and in previous pharmacophore models for CYP2D6 or two different orientations for Asp301.[3,9,10] The resulting pharmacophore model is depicted in Figure 5. The larger 10 Å compounds extending from the overall domain occupied by the remaining compounds used to derive the pharmacophore model are clearly visible. These compounds were superimposed on top of each other, thereby maximizing the superposition of the parts extending from the overall pharmacophore model and can interact with Glu216 instead of Asp301.

The homology model (Figure 6) could explain all known experimental data for CYP2D6[27,29,45,46] and had the amino acids which were identified by site-directed mutagenesis as being responsible for important substrate−protein interactions in other 2-family P450s[26] surrounding the active site. The current alignment (Figure 2) identified a variety of β-sheets in the C-terminal domain not present in the previous protein model[26] (structural elements are highlighted in Figure 2). One of the key elements of homology modeling is the accuracy of the sequence alignment. Although the sequence similarity between the P450 families is low,[1] the structural similarity of all significant secondary structural elements is conserved across the available bacterial structures. It is believed that this structural homology is also conserved in the membrane-bound mammalian P450s,[47,48] and therefore modeling of the conserved core should be reliable. However, a few regions, most notably the region between the B- and C-helices, are diverse in terms of both structure and sequence across the available P450 crystal structures. Given the lack of sequence and structural homology between the bacterial crystal structures, with other P450 sequences in this region, modeling of these regions will remain speculative.

MO calculations alone could in general not reliably predict the metabolic site of oxidation, as oxidation next to either a nitrogen or oxygen atom is most favored. Only in most cases where the substrate is O-dealkylated (**2**, **6**, **8**, **11**, **13**, **14**, **18**, **21**, **23**, **24**, **31**, **38**, and **40**) does the site of oxidation coincide with the most stable product. However, when taking into account the distance constraints imposed by CYP2D6 (a distance of 5, 7, or 10 Å between site of oxidation and basic nitrogen atom[3−5]), it was possible to identify the metabolic products based on the relative stability of the various hydroxylated species. In the case of predictions based on the model, the MO results for the various possible products will be used to guide the modeling, thereby enhancing the importance of these MO calculations.

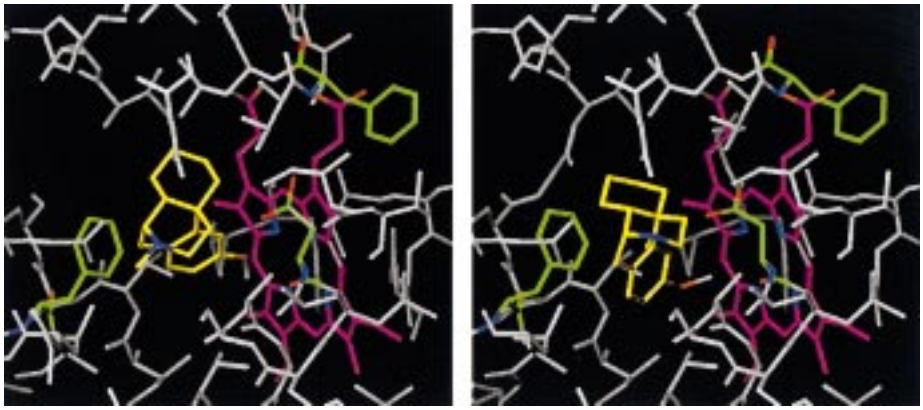

Figure 4. Orientation of compound **2** (taken from the pharmacophore model) docked into the active site of the protein model for CYP2D6 (left) before minimization in the presence of the protein and (right) after minimization in the presence of the protein. The heme moiety is indicated in pink, and dextromethorphan (**2**) is shown in yellow, while Phe120, Asp301, and Phe481 are highlighted in green.

Figure 5. Initial pharmacophore model for CYP2D6. No protein influences taken into account. Sites of oxidation are shown in white, while (basic) nitrogen atoms are shown in blue.

Direct insertion of the pharmacophore model for 5 and 7 Å substrates (Figure 5) into the protein model (Figure 6) was possible without steric clashes between substrates and protein. As the two models were derived independently, the high level of complementarity of the models can be interpreted as a cross-validation. The site of oxidation was positioned 3−3.5 Å above the iron of the heme with the plane of the heme roughly perpendicular to the planar region of the pharmacophore model. However, the interaction between the basic nitrogen atom and the carboxylate moiety of Asp301 was not optimal. The compounds which extended considerably (compounds **3**, **6**, **25**, and **36**−**39**) did fit in the active site of the protein model and could interact with Glu216.

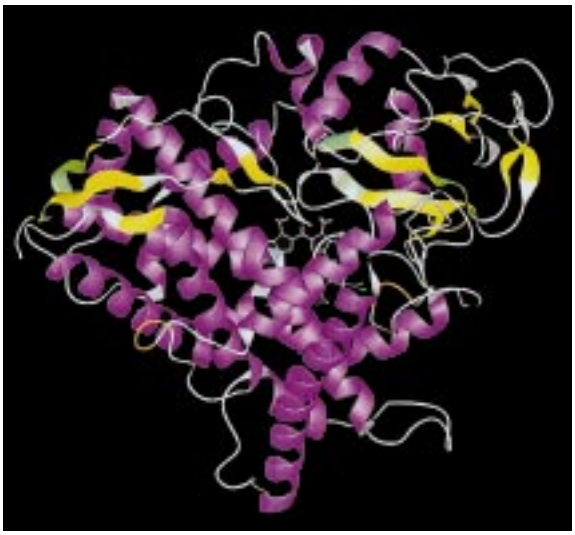

Figure 6. Protein model for CYP2D6. Secondary structure elements are shown as α-helices in purple and *β*-sheets in yellow.

Minimization of each individual substrate within the protein[44,49] optimized the distance between the basic nitrogen atom and the carboxylic acid side chain of either Asp301 (for the 5 and 7 Å substrates) or Glu216 (for the 10 Å substrates), while inducing only minor changes on the overall pharmacophore model (Figure 7). The most remarkable differences are visible when examining the pharmacophore model from a top view (Figures 5, bottom, and 7, bottom). Although the planarity of the region around the site of oxidation is slightly reduced, the various substrates extending toward the top become more clustered due to an interaction with Phe481 (e.g., compound **5** (dark green) extending considerably in Figure 5, bottom, is grouped together with several other compounds after minimization in Figure 7, bottom). Several specific substrates which extend from the overall volume of the pharmacophore model in Figure 5, bottom are compound **3** (benzylic hydroxylation, light green) at the top of the model, compound **9** (light green) at the bottom of the model, and compound **34** (orange) close to the site of oxidation. After minimization these extending substrates are incorporated in several distinct groups of substrates (Figure 7, bottom). The side view confirms

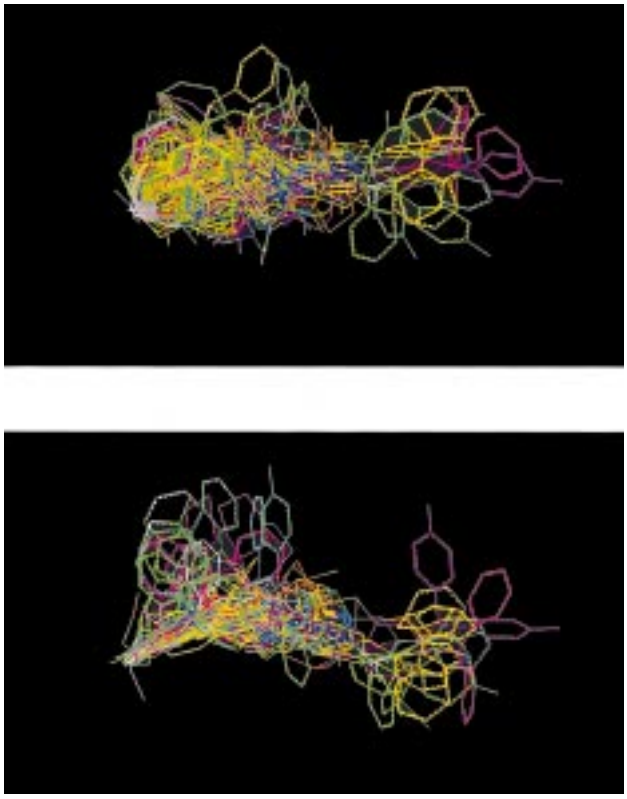

Figure 7. Substrate region of the combined pharmacophore−protein model. Orientations of the various substrates are shown after (constrained) geometry optimization within the CYP2D6 active site. Each substrate was independently energy-minimized in the active site of the protein model starting from the orientation shown in Figure 5. Sites of oxidation are shown in white, while (basic) nitrogen atoms are shown in blue.

that the overlay of the substrates is improved by the minimization in the protein (compare Figures 5, top, and 7, top).

When all substrates were subsequently submitted to an AM1 geometry optimization (starting from the orientation resulting from the geometry optimization in the presence of the protein (Figure 7)), there were only very minor changes in substrate geometry. This indicates that the conformations in the protein are low-energy conformations and not a result of protein-imposed steric restrictions. It was, however, still possible to incorporate all substrates within the active site region of the homology model, and the energy differences between these AM1-optimized geometries and the AM1 energies for the global minimum were generally less than 5 kcal/mol (0−10.4 kcal/mol).

Conclusions

To derive a model capable of explaining and predicting metabolism catalyzed by an enzyme, neither a pharmacophore model, a protein model, nor molecular orbital calculation on their own will result in a reliable model. The pharmacophore model identifies similarities between different substrates and suggests possible common interactions but ignores the steric and electronic influence of the protein. Docking molecules into a protein model takes into account the steric and electronic influence of the protein but will generally result in a variety of orientations for each substrate in the active site of the protein, which makes it difficult to reproduce. By using a single orientation of each compound, superimposing these together in a pharmacophore model, and docking these into a protein model, a reproducible and well-defined combined model results which incorporates more experimental data than each model separately. Therefore, a combination of these two approaches (pharmacophore modeling and protein modeling) will result in a more well-defined and reproducible model which will take into account not only the similarities between the various substrates but also the steric and electronic properties of the surrounding enzyme. Molecular orbital calculations can identify the chemically most likely intermediates and products based on internal energies; however, the steric and electronic influences of the protein, which distinguish the catalyzed reaction from the chemical reaction, are ignored. When predicting the possible metabolism of newly designed compounds, these calculations are very useful in indicating the most reactive parts of the compound and indicate possible sites of metabolism. However, only when combining all three methods into one approach does predicting metabolism become feasible.

Work is in progress to test the constructed model with a variety of compounds (both substrates and nonsubstrates of CYP2D6). In this case the MO results for the various possible products will be used to guide the modeling, thereby enhancing the importance of the MO calculations. In addition, the incorporation of other metabolic pathways catalyzed by CYP2D6, like the N-dealkylation of deprenyl,[50] into the combined model is also under investigation.

Acknowledgment. Dr. M. J. Sutcliffe is gratefully acknowledged for providing the Modeler input required to enable the inclusion of the heme moiety in the protein modeling.

References

(1) Nelson, D. R.; Koymans, L.; Kamataki, T.; Stegeman, J. J.; Feyereisen, R.; Waxman, D. J.; Waterman, M. R.; Gotoh, O.; Coon, M. J.; Estabrook, R. W.; Gunsalus, I. C.; Nebert, D. W. P450 superfamily: update on new sequences, gene mapping, accession numbers and nomenclature. *Pharmacogenetics* **1996**, *6*, 1−42.

(2) Daly, A. K.; Brockmöller, J.; Broly, F.; Eichelbaum, M.; Evans, W. E.; Gonzalez, F. J.; Huang, J. D.; Idle, J. R.; Ingelman-Sundberg, M.; Ishizaki, T.; Jacqz-Aigrain, E.; Meyer, U. A.; Nebert, D. W.; Steen, V. M.; Wolf, C. R.; Zanger, U. M. Nomenclature for human *CYP2D6* alleles. *Pharmacogenetics* **1996**, *6*, 193−201.

(3) Koymans, L. M. H.; Vermeulen, N. P. E.; van Acker, S. A. B. E.; te Koppele, J. M.; Heykants, J. J. P.; Lavrijsen, K.; Meuldermans, W.; Donné-Op den Kelder, G. M. A predictive model for substrates of cytochrome P-450-debrisoquine (2D6). *Chem. Res. Toxicol.* **1992**, *5*, 211−219.

(4) Strobl, G. R.; von Kreudener, S.; Stöckigt, J.; Guengerich, F. P.; Wolff, T. Development of a pharmacophore for inhibition of human liver cytochrome P-450 2D6: molecular modelling and inhibition studies. *J. Med. Chem.* **1993**, *36*, 1136−1145.

(5) de Groot, M. J.; Bijloo, G. J.; Martens, B. J.; van Acker, F. A. A.; Vermeulen, N. P. E. A refined substrate model for human cytochrome P450 2D6. *Chem. Res. Toxicol.* **1997**, *10*, 41−48.

(6) Wolff, T.; Distlerath, L. M.; Worthington, M. T.; Groopman, J. D.; Hammons, G. J.; Kadlubar, F. F.; Prough, R. A.; Martin, M. V.; Guengerich, F. P. Substrate specificity of human liver cytochrome P-450 debrisoquine hydroxylase probed using immunochemical inhibition and chemical modeling. *Cancer Res.* **1985**, *45*, 2116−2122.

(7) Meyer, U. A.; Gut, J.; Kronbach, T.; Skoda, C.; Meier, U. T.; Catin, T.; Dayer, P. The molecular mechanism of two common polymorphisms of drug oxidation. Evidence for functional changes in cytochrome P-450 isozymes catalysing bufuralol and mephenytoin oxidation. *Xenobiotica* **1986**, *16*, 449−464.

(8) Islam, S. A.; Wolf, C. R.; Lennard, M. S.; Sternberg, M. J. E. A three-dimensional molecular template for substrates of human cytochrome P450 involved in debrisoquine 4-hydroxylation. *Carcinogenesis* **1991**, *12*, 2211−2219.
(9) de Groot, M. J.; Bijloo, G. J.; Hansen, K. T.; Vermeulen, N. P. E. Computer prediction and experimental validation of cytochrome P450-2D6 dependent oxidation of GBR 12909 (1-[2-[bis-(4-fluorophenyl)methoxy]ethyl]-4-(3-phenylpropyl)piperazine). *Drug Metab. Dispos.* **1995**, *23*, 667−669.
(10) de Groot, M. J.; Bijloo, G. J.; van Acker, F. A. A.; Fonseca Guerra, C.; Snijders, J. G.; Vermeulen, N. P. E. Extension of a predictive substrate model for human cytochrome P4502D6. *Xenobiotica* **1997**, *27*, 357−368.
(11) Poulos, T. L. Cytochrome P450. *Curr. Opin. Struct. Biol.* **1995**, *5*, 767−774.
(12) Poulos, T. L.; Finzel, B. C.; Gunsalus, I. C.; Wagner, G. C.; Kraut, J. The 2.6-Å crystal structure of *Pseudomonas putida* cytochrome P-450. *J. Biol. Chem.* **1985**, *260*, 16122−16130.
(13) Poulos, T. L.; Finzel, B. C.; Howard, A. J. High-resolution crystal structure of cytochrome P450cam. *J. Mol. Biol.* **1987**, *195*, 687−700.
(14) Ravichandran, K. G.; Boddupalli, S. S.; Hasemann, C. A.; Peterson, J. A.; Deisenhofer, J. Crystal structure of hemoprotein domain of P450 μ_B-3, a prototype for microsomal P450s. *Science* **1993**, *261*, 731−736.
(15) Li, H.; Poulos, T. L. Modeling protein-substrate interactions in the heme domain of cytochrome $P450_{BM-3}$. *Acta Crystallogr. Sect. D-Biol. Crystallogr.* **1995**, *51*, 21−32.
(16) Cupp-Vickery, J. R.; Li, H. Y.; Poulos, T. L. Preliminary crystallographic analysis of an enzyme involved in erythromycin biosynthesis: Cytochrome P450eryF. *Proteins: Struct. Funct. Genet.* **1994**, *20*, 197−201.
(17) Cupp-Vickery, J. R.; Poulos, T. L. Structure of cytochrome P450eryF involved in erythromycin biosynthesis. *Nature Struct. Biol.* **1995**, *2*, 144−153.
(18) Hasemann, C. A.; Ravichandran, K. G.; Peterson, J. A.; Deisenhofer, J. Crystal structure and refinement of cytochrome $P450_{terp}$ at 2.3 Å resolution. *J. Mol. Biol.* **1994**, *236*, 1169−1185.
(19) Park, S.-Y.; Shimizu, H.; Adachi, S.; Shiro, Y.; Iizuka, T.; Nakagawa, A.; Tanaka, I.; Shoun, H.; Hori, H. Crystalization, preliminary diffraction and electron paramagnetic resonance studies of a single crystal of cytochrome P450nor. *FEBS Lett.* **1997**, *412*, 346−350.
(20) Park, S.-Y.; Shimizu, H.; Adachi, S.; Shiro, Y.; Iizuka, T.; Shoun, H. Crystal structure of nitric oxide reductase cytochrome P-450nor from *Fusarium oxysporum*. *Keio University Symp. Life Sci. Med.* **1998**, *1 (Oxygen Homeostasis and Its Dynamics)*, 147−155.
(21) Obayashi, E.; Tsukamoto, K.; Adachi, S.; Takahashi, S.; Nomura, M.; Iizuka, T.; Shoun, H.; Shiro, Y. Unique binding of nitric oxide to ferric nitric oxide reductase from *Fusarium oxysporum* elucidated with infrared, resonance Raman, and X-ray absorption spectroscopies. *J. Am. Chem. Soc.* **1997**, *119*, 7807−7816.
(22) de Groot, M. J.; Vermeulen, N. P. E. Modeling the active site of cytochrome P450s and glutathione *S*-transferases, two of the most important biotransformation enzymes. *Drug Metab. Rev.* **1997**, *29*, 747−799.
(23) Koymans, L. M. H.; Vermeulen, N. P. E.; Baarslag, A.; Donné-Op den Kelder, G. M. A preliminary 3D model for cytochrome P450 2D6 constructed by homology model building. *J. Comput.-Aided Mol. Des.* **1993**, *7*, 281−289.
(24) Lewis, D. F. V. Three-dimensional models of human and other mammalian microsomal P450s constructed from an alignment with CYP102 ($P450_{bm3}$). *Xenobiotica* **1995**, *25*, 333−366.
(25) Modi, S.; Paine, M. J.; Sutcliffe, M. J.; Lian, L. Y.; Primrose, W. U.; Wolf, C. R.; Roberts, G. C. K. A model for human cytochrome P_{450} 2D6 based on homology modeling and NMR studies of substrate binding. *Biochemistry* **1996**, *35*, 4540−4550.
(26) de Groot, M. J.; Vermeulen, N. P. E.; Kramer, J. D.; van Acker, F. A. A.; Donné-Op den Kelder, G. M. A three-dimensional protein model for human cytochrome P450 2D6 based on the crystal structures of P450 101, P450 102 and P450 108. *Chem. Res. Toxicol.* **1996**, *9*, 1079−1091.
(27) Ellis, S. W.; Rowland, K.; Ackland, M. J.; Rekka, E.; Simula, A. P.; Lennard, M. S.; Wolf, C. R.; Tucker, G. T. Influence of amino acid residue 374 of cytochrome P450 2D6 (CYP2D6) on the regio- and enantioselective metabolism of metoprolol. *Biochem. J.* **1996**, *316*, 647−654.
(28) Lewis, D. F. V.; Eddershaw, P. J.; Goldfarb, P. S.; Tarbit, M. H. Molecular modelling of cytochrome P4502D6 (CYP2D6) based on an alignment with CYP102: structural studies on specific CYP2D6 substrate metabolism. *Xenobiotica* **1997**, *27*, 319−340.
(29) Ellis, S. W.; Hayhurst, G. P.; Smith, G.; Lightfoot, T.; Wong, M. M. S.; Simula, A. P.; Ackland, M. J.; Sternberg, M. J. E.; Lennard, M. S.; Tucker, G. T.; Wolf, C. R. Evidence that aspartic acid 301 is a critical substrate-contact residue in the active site of cytochrome P450 2D6. *J. Biol. Chem.* **1995**, *270*, 29055−29058.
(30) Allan, F. H.; Kennard, O. 3D search and research using the Cambridge Structural Database. *Chem. Des. Automat. News* **1993**, *8*, 31−37.
(31) Spartan, 1996, SGI version 4.1.1 OpenGL; Wavefunction Inc., Irvine, CA 92715.
(32) Conformational search using the SYBYL force field employing the genetic algorithm, without geometry optimization (popsize = 150−250 depending on number of rotable bonds). Of the resulting conformers, all conformers within 25 kcal/mol from the lowest energy were geometry-optimized using AM1 (optcycle = 1000, maxcycle = 1000).
(33) Dewar, M. J. S.; Zoebisch, E. G.; Healy, E. F.; Stewart, J. J. P. AM1: a new general purpose quantum mechanical molecular model. *J. Am. Chem. Soc.* **1985**, *107*, 3902−3909.
(34) The distances were kept fixed at the values derived from the AM1 energy-minimized structures (Table 1).
(35) SYBYL, 1997, version 6.4; Tripos Inc., St. Louis, MO 63144-2913.
(36) Several X-ray structures (Protein Data Bank) are available for CYP101 and CYP102. For CYP101 the 2CPP crystal structure was used, for CYP102 monomer A of the crystal structure 2HPD was used, while for CYP108 the crystal structure 1CPT was used.
(37) Quanta97, 1998, version 97.0305; Molecular Simulations Inc., San Diego, CA 92121-3752.
(38) de Groot, M. J. Computational Chemistry and Molecular Modeling Approaches to Biotransformation Enzymes. Enzyme Mechanisms, Substrate and Protein Models of Cytochrome P450 and Glutathione *S*-Transferase Isoenzymes. Thesis, Vrije Universiteit Amsterdam, The Netherlands, 1996.
(39) Presentation by Dr. S. W. Ellis at the Symposium on Molecular Modelling of Drug Metabolizing Enzymes, British Pharmacological Society Winter Meeting, Dec 10−12, 1997, Harrogate International Centre.
(40) Smith, G.; Modi, S.; Pillai, I.; Lian, L.-Y.; Suthcliffe, M. J.; Pritchard, M. P.; Friedberg, T.; Roberts, G. C. K.; Wolf, C. R. Determinants of the substrate specificity of human cytochrome P-450 CYP2D6: design and construction of a mutant with testosterone hydroxylase activity. *Biochem. J.* **1998**, *331*, 783−792.
(41) There are inconsistencies in the literature in the naming of the pyrrole rings of the heme moiety. Here, the crystallographer's nomenclature is used for the heme moiety.
(42) Laskowski, R. A.; McArthur, M. W.; Moss, D. S.; Thornton, J. M. PROCHECK: A program to check the stereochemical quality of protein structures. *J. Appl. Crystallogr.* **1993**, *26*, 283−291.
(43) GBR-12,909 (**3**) has two basic nitrogen atoms: one at ∼7 Å and a second at ∼10 Å from the site of oxidation (aromatic hydroxylation).
(44) Minimization options: SYBYL force field, Powell minimization with standard minimize details. Termination on gradient <0.1 kcal/(mol·Å), with as many iterations as required for convergence. Constraints: iron−site of oxidation 3.0 Å (constant = 200) and basic nitrogen atom−Asp301 carboxylate oxygen or basic nitrogen atom−Glu216 carboxylate oxygen 2.7 Å (constant = 100).
(45) Ellis, S. W.; Rowland, K.; Harlow, J. R.; Simula, A. P.; Lennard, M. S.; Woods, H. F.; Tucker, G. T.; Wolf, C. R. Regio- and enantioselective metabolism of metoprolol by two human cDNA-derived CYP2D6 proteins. *Br. J. Pharmacol.* **1994**, *112*, 244P.
(46) Ellis, S. W.; Hayhurst, G. P.; Harlow, J. R.; Lennard, M. S.; Tucker, G. T.; Simula, A. P.; Smith, G.; Wolf, C. R. Catalytic function of aspartic acid 301 in debrisoquine 4-hydroxylase cytochrome P450 (CYP2D6). *Br. J. Clin. Pharmacol.* **1995**, *40*, 178P−179P.
(47) Nelson, D. R.; Strobel, H. W. Secondary structure prediction of 52 membrane-bound cytochromes P450 shows a strong structural similarity to $P450_{cam}$. *Biochemistry* **1989**, *28*, 656−660.
(48) Gotoh, O. Substrate recognition sites in cytochrome P450 family 2 (CYP2) proteins inferred from comparative analyses of amino acid and coding nucleotide sequences. *J. Biol. Chem.* **1992**, *267*, 83−90.
(49) In the protein, only Glu216, Asp301, and Phe481 are allowed to reorientate in reaction to the presence of the substrate.
(50) Grace, J. M.; Kinter, M. T.; MacDonald, T. L. Atypical metabolism of deprenyl and its enantiomer, (S)-(+)-N,α-dimethyl-N-propynylphenethylamine, by cytochrome P450 2D6. *Chem. Res. Toxicol.* **1994**, *7*, 286−290.
(51) Hasemann, C. A.; Kurumbail, R. G.; Boddupalli, S. S.; Peterson, J. A.; Deisenhofer, J. Structure and function of cytochromes P450: a comparative analysis of three crystal structures. *Structure* **1995**, *2*, 41−62.
(52) Wolff, T.; Distlerath, L. M.; Worthington, M. T.; Guengerich, F. P. Human liver debrisoquine 4-hydroxylase: test for specificity toward various monooxygenase substrates and model of the active site. *Arch. Toxicol.* **1987**, *60*, 89−90.

(53) Lightfoot, T.; Ellis, S. W.; Mahling, J.; Ackland, M. J.; Blaney, F.; Bijloo, G. J.; de Groot, M. J.; Vermeulen, N. P. E.; Blackburn, G. M.; Lennard, M. S.; Tucker, G. T. Regioselective hydroxylation of debrisoquine by cytochrome P450 2D6. Rationalization by active site modeling and mechanism of oxidation. *Pharmacogenetics*, **1999**, submitted for publication.
(54) Küpfer, A.; Schmid, B.; Pfaff, G. Pharmacogenetics of dextromethorphan O-demethylation in man. *Xenobiotica* **1986**, *16*, 421−433.
(55) Coutts, R. T.; Bach, M. V.; Baker, G. B. Metabolism of amitriptyline with CYP2D6 expressed in a human cell line. *Xenobiotica* **1997**, *27*, 33−47.
(56) Ebner, T.; Eichelbaum, M. The metabolism of aprindine in relation to the sparteine/debrisoquine polymorphism. *Br. J. Clin. Pharmacol.* **1993**, *35*, 426−430.
(57) Feifel, N.; Kucher, K.; Fuchs, L.; Jedrychowski, M.; Schmidt, E.; Antonin, K. H.; Bieck, P. R.; Gleiter, C. H. Role of cytochrome P4502D6 in the metabolism of brofaromine. A new selective MAO-A inhibitor. *Eur. J. Clin. Pharmacol.* **1993**, *45*, 265−269.
(58) Mautz, D. S.; Nelson, W. L.; Shen, D. D. Regioselective and stereoselective oxidation of metoprolol and bufuralol catalyzed by microsomes containing cDNA-expressed human P4502D6. *Drug Metab. Dispos.* **1995**, *23*, 513−517.
(59) Oldham, H. G.; Clarke, S. E. In vitro identification of the human cytochrome P450 enzymes involved in the metabolism of R(+)- and S(−)-carvedilol. *Drug Metab. Dispos.* **1997**, *25*, 970−977.
(60) Narimatsu, S.; Kariya, S.; Isozaki, S.; Ohmori, S.; Kitada, M.; Hosokawa, S.; Masubuchi, Y.; Suzuki, T. Involvement of CYP2D6 in oxidative metabolism of cinnarizine and flunarizine in human liver microsomes. *Biochem. Biophys. Res. Commun.* **1993**, *193*, 1262−1268.
(61) Nielsen, K. K.; Brøsen, K.; Hansen, M. G. J.; Gram, L. F. Single-dose kinetics of clomipramine: relationship to the spartein and *S*-mephenytoin oxidation polymorphisms. *Clin. Pharmacol. Ther.* **1994**, *55*, 518−527.
(62) Dayer, P.; Desmeules, J.; Leemann, T.; Striberni, R. Bioactivation of the narcotic drug codeine in human liver is mediated by the polymorphic monooxygenase catalyzing debrisoquine 4-hydroxylation (cytochrome P-450 db1/bufI). *Biochem. Biophys. Res. Commun.* **1988**, *152*, 411−416.
(63) Su, P.; Coutts, R. T.; Baker, G. B.; Daneshtalab, M. Analysis of imipramine and three metabolites produced by isozyme CYP2D6 expressed in a human cell line. *Xenobiotica* **1993**, *23*, 1289−1298.
(64) Kirkwood, L. C.; Nation, R. L.; Somogyi, A. A. Characterization of the human cytochrome P450 involved in the metabolism of dihydrocodeine. *Br. J. Clin. Pharmacol.* **1997**, *44*, 549−555.
(65) Liu, Z.; Mortimer, Ø.; Smith, C. A. D.; Wolf, C. R.; Rane, A. Evidence for a role of cytochrome P450 2D6 and 3A4 in ethylmorphine metabolism. *Br. J. Clin. Pharmacol.* **1995**, *39*, 77−80.
(66) Fischer, V.; Vogels, B.; Maurer, G.; Tynes, R. E. The antipsychotic clozapine is metabolized by the polymorphic human microsomal and recombinant cytochrome P450 2D6. *J. Pharmacol. Exp. Ther.* **1992**, *260*, 1355−1360.
(67) Jack, D. B.; Stenlake, J. B.; Templeton, R. The metabolism and excretion of guanoxan in man. *Xenobiotica* **1972**, *2*, 35−43.
(68) Kaplan, H. L.; Busto, U. E.; Baylon, G. J.; Cheung, S. W.; Otton, S. V.; Somer, G.; Sellers, E. M. Inhibition of cytochrome P450 2D6 metabolism of hydrocodone to hydromorphone does not importantly affect abuse liability. *J. Pharmacol. Exp. Ther.* **1997**, *281*, 103−108.
(69) Pierce, D. M.; Smith, S. E.; Franklin, R. A. The pharmacokinetics of indoramin and 6-hydroxyindoramin in poor and extensive hydroxylators of debrisoquine. *Eur. J. Clin. Pharmacol.* **1987**, *33*, 59−65.
(70) Tucker, G. T.; Lennard, M. S.; Ellis, S. W.; Woods, H. F.; Cho, A. K.; Lin, L. Y.; Hiratsuka, A.; Smitz, D. A.; Chu, T. Y. Y. The demethylation of methylenedioxymethamphetamine ("Ecstasy") by debrisoquine hydrolase (CYP2D6). *Biochem. Pharmacol.* **1994**, *47*, 1151−1156.
(71) Lin, J. H.; Lu, A. Y. H. *Inhibition of cytochrome P-450 and implications in drug development*; Academic Press: New York, 1997; pp 295−304.
(72) Wu, D.; Otton, S. V.; Inaba, T.; Kalow, W.; Sellers, E. M. Interactions of amphetamine analogues with human liver CYP2D6. *Biochem. Pharmacol.* **1997**, *53*, 1605−1612.
(73) Geertsen, S.; Foster, B. C.; Wilson, D. L.; Cyr, T. D.; Casley, W. Metabolism of methoxyphenamine and 2-methoxyamphetamine in P4502D6-transfected cells and cell preparations. *Xenobiotica* **1995**, *25*, 895−906.
(74) Broly, F.; Libersa, C.; Lhermitte, M.; Dupuis, B. Inhibitory studies of mexiletine and dextromethorphan oxidation in human liver microsomes. *Biochem. Pharmacol.* **1990**, *39*, 1045−1053.
(75) Koyama, E.; Chiba, K.; Tani, M.; Ishizaki, T. Identification of human cytochrome P450 isoforms involved in the stereoselective metabolism of mianserin enantiomers. *J. Pharmacol. Exp. Ther.* **1996**, *278*, 21−30.
(76) Dahl, M. L.; Voortman, G.; Alm, C.; Elwin, C. E.; Delbressine, L.; Vos, R.; Bogaards, J. J. P.; Bertilsson, L. In vitro and in vivo studies on the disposition of mirtazapine in humans. *Clin. Drug Invest.* **1997**, *13*, 37−46.
(77) Olesen, O. V.; Linnet, K. Hydroxylation and demethylation of the tricyclic antidepressant nortriptyline by cDNA-expressed human cytochrome P-450 isozymes. *Drug Metab. Dispos.* **1997**, *25*, 740−744.
(78) Fischer, V.; Vickers, A. E. M.; Heitz, F.; Mahadevan, S.; Baldeck, J. P.; Minery, P.; Tynes, R. The polymorphic cytochrome P-4502D6 is involved in the metabolism of both 5-hydroxytryptamine antagonists, tropisetron and ondansetron. *Drug Metab. Dispos.* **1994**, *22*, 269−274.
(79) Sindrup, S. H.; Brøsen, K.; Gram, L. F.; Hallas, J.; Skjelbo, E.; Allen, A.; Allen, G. D.; Cooper, S. M.; Mellows, G.; Tasker, T. C. G.; Zussman, B. D. The relationship between paroxetine and the sparteine oxidation polymorphism. *Clin. Pharmacol. Ther.* **1992**, *51*, 278−287.
(80) Amoah, A. G. B.; Gould, B. J.; Parke, D. V.; Lockhart, J. D. F. Further studies on the pharmacokinetics of perhexiline maleate in humans. *Xenobiotica* **1986**, *16*, 63−68.
(81) Gould, B. J.; Amoah, A. G. B.; Parke, D. V. Stereoselective pharmacokinetics of perhexiline. *Xenobiotica* **1986**, *16*, 491−502.
(82) Eichelbaum, M. Polymorphic drug oxidation in humans. *Fed. Proc.* **1989**, *43*, 2298−2302.
(83) Kroemer, H. K.; Fischer, C.; Meese, C. O.; Eichelbaum, M. Enantiomer/enantiomer interaction of (*S*)- and (*R*)-propafenon for cytochrome P450IID6-catalyzed 5-hydroxylation: in vitro evaluation of the mechanism. *Mol. Pharmacol.* **1991**, *40*, 135−142.
(84) Botsch, S.; Gautier, J.-C.; Beaune, P.; Eichelbaum, M.; Kroemer, H. K. Identification and characterization of the cytochrome P450 enzymes involved in *N*-dealkylation of propafenon: molecular base for interaction potential and variable disposition of active metabolites. *Mol. Pharmacol.* **1993**, *43*, 120−126.
(85) Yoshimoto, K.; Echizen, H.; Chiba, K.; Tani, M.; Ishizaki, T. Identification of human CYP isoforms involved in the metabolism of propranolol enantiomers. *N*-desisopropylation is mediated mainly by CYP1A2. *Br. J. Clin. Pharmacol.* **1995**, *39*, 421−431.
(86) Rowland, K.; Ellis, S. W.; Lennard, M. S.; Tucker, G. T. Variable contribution of CYP2D6 to the N-dealkylation of S-(−)-propranolol by human liver micriosomes. *Br. J. Clin. Pharmacol.* **1996**, *42*, 390−393.
(87) Kupfer, D.; Mani, C.; Lee, C. A.; Rifkind, A. B. Induction of tamoxifen-4-hydroxylation by 2,3,7,8-tetrachlorodibenzo-*p*-dioxin (TCDD), β-naphthoflavone (βNF), and phenobarbital (PB) in avian liver: identification of P450 $TCDD_{AA}$ as catalyst of 4-hydroxylation induced by TCDD and βNF. *Cancer Res.* **1994**, *54*, 3140−3144.
(88) Crewe, H. K.; Ellis, S. W.; Lennard, M. S.; Tucker, G. T. Variable contribution of cytochromes P450 2D6, 2C9 and 3A4 to the 4-hydroxylation of tamoxifen by human liver microsomes. *Biochem. Pharmacol.* **1997**, *53*, 171−178.
(89) Jones, B. C.; Hyland, R.; Ackland, M. J.; Tyman, C. A.; Smith, D. A. Interaction of terfenadine and its primary metabolites with cytochrome P450 2D6. *Drug Metab. Dispos.* **1998**, *26*, 875−882.
(90) Berndt, A.; Hoffmann, C.; Richter, K.; Oertel, R.; Vierkant, A.; Siegmund, W. Tiracizine disposition in healthy volunteers with reference to the debrisoquine oxidation phenotype. *Br. J. Clin. Pharmacol.* **1995**, *40*, 287−288.
(91) Ball, S. E.; Ahern, D.; Scatina, J.; Kao, J. Venlafaxine: in vitro inhibition of CYP2D6 dependent imipramine and desipramine metabolism; comparative studies with selected SSRIs, and effects on human hepatic CYP3A4, CYP2C9 and CYP1A2. *Br. J. Clin. Pharmacol.* **1997**, *43*, 619−626.

JM981118H